Multiple Andreev Reflections Revealed by the Energy Distribution of Quasiparticles

F. Pierre, A. Anthore, H. Pothier, C. Urbina, and D. Esteve

Service de Physique de l'Etat Condensé, Commissariat à l'Energie Atomique, Saclay, F-91191 Gif-sur-Yvette Cedex, France
(Received 13 October 2000)

We have performed the tunnel spectroscopy of the energy distribution function of quasiparticles in 5-μm-long silver wires connected to superconducting reservoirs biased at different potentials. The distribution function $f(E)$ presents several steps, which are manifestations of multiple Andreev reflections at the NS interfaces. The rounding of the steps is well explained by electron-electron interactions.

The modification of the properties of a normal (i.e., non-superconducting) metallic electrode when it is connected to a superconducting one, a phenomenon called "proximity effect," has been highlighted by experiments on mesoscopic devices [1]. In metallic nanostructures, equilibrium properties, such as the density of states [2], the conductivity [3], or the supercurrent [4], are now well explained. The propagation of the correlations between time-reversed states from a superconductor (S) into a diffusive normal metal (N) is described by the Usadel equations [5], which apply to situations where all superconductors are at the same potential. In this Letter, we address an out-of-equilibrium situation, in which two superconductors connected through a long ($L \simeq 5\ \mu$m), diffusive normal wire are biased at different potentials (see Fig. 1). We have measured the energy distribution function of quasiparticles in the middle of the wire, which is expected to be strongly modified by the presence of superconductors at the ends, since quasiparticles can escape the wire only if their energy exceeds the energy gap Δ of the superconductor. Therefore, in the presence of a finite voltage across the wire, the quasiparticles in the wire are expected to be "heated" up to the gap energy [6]. A quantitative description follows from the concept of multiple Andreev reflections, which recently has been shown to describe in great detail the current-voltage characteristics [7], the noise [8], and the supercurrent [9] in atomic point contacts between superconductors. An Andreev reflection consists of the reflection of a quasielectron into a quasihole (or vice versa) at the N side of an NS interface, a process which transfers a Cooper pair into the superconductor. The energies of the two quasiparticles involved are symmetrical with regard to the electrochemical potential of the superconductor. When two superconductors are present, successive Andreev reflections at both superconductors lead to a progressive rise of the quasiparticle energies, till the superconducting gap is exceeded. At zero voltage, multiple Andreev reflections lead to the formation of bound states which carry the supercurrent [10]; at finite voltage, they result in nonlinearities in the current voltage characteristics [6,7]. Here, we focus on the fingerprint of multiple Andreev reflections in the shape of the energy distribution function $f(E)$ of the quasiparticles.

For simplicity, we first make the following assumptions: (i) electron-electron and electron-phonon interactions are neglected; (ii) the renormalization of the diffusion constant in the normal wire by proximity effect is neglected; (iii) the probability of Andreev reflection is taken equal to 1 for quasiparticle energies within the gap, and to 0 elsewhere. Under assumptions (i) and (ii), the distribution function varies linearly with the position X along the wire [11]. Because of Andreev reflection, the occupation factor for quasielectrons and quasiholes at symmetrical energies about the electrochemical potential μ of the superconductor is equal at the NS interfaces, as well as their gradients.
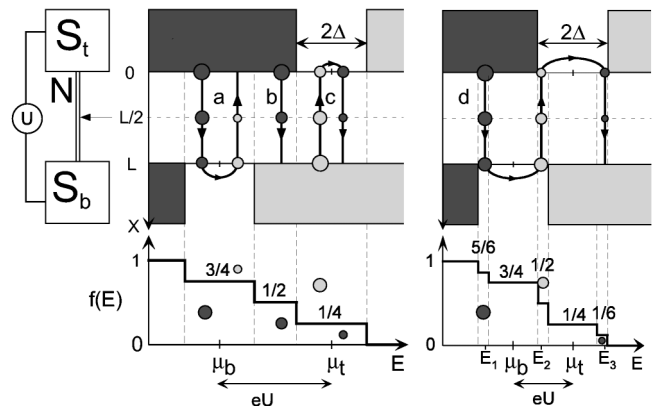
FIG. 1. Left: layout of the experiment: a voltage U is applied between two superconductors (S) connected through a normal wire (N) of length L. A superconducting probe electrode, represented by an arrow, forms a tunnel junction with the central part of the wire. Top center and top right: representation in the energy (horizontal axis) and position (vertical axis) space of the quasiparticle paths responsible for the current through the normal wire. The excitation spectrum of the top and bottom superconductors has a gap 2Δ centered on their electrochemical potentials μ_t and μ_b ($\mu_t - \mu_b = eU$), with quasielectron states occupied at negative energies (dark areas) and empty (light gray areas) at positive energies. Quasiparticle paths consist of quasielectron (dark disks) and quasihole (light gray disks) trajectories at symmetric energies about μ_t or μ_b, connected by Andreev reflection. The area of the disks is proportional to the occupation factor of the quasiparticle state, which varies linearly along the path from 1 to 0. The bottom plots are the energy distribution functions at the center of the wire, at $eU > 2\Delta$ (center) and $\Delta < eU < 2\Delta$ (right).

One can therefore define quasiparticle paths in the energy-position space between occupied and empty quasiparticle states in the superconductors, along which both the nature of the quasiparticle and its energy change at each NS interface. The occupancy f of the quasiparticle state on this diffusive path varies continuously from 1 to 0 along the trajectory, with a gradient given by the inverse of the length of the trajectory. Hence, f is simply, at a given point of a trajectory, the remaining fraction of the path. The distribution function $f(E)$, which is defined for quasielectrons, is then equal to f at a point where the quasiparticle on the considered trajectory is a quasielectron, and to $1 - f$ where it is a quasihole. This allows one to determine the distribution function as a function of energy and position in the wire. Two examples are illustrated in Fig. 1. In the first one, the voltage $U = (\mu_t - \mu_b)/e$ is larger than $2\Delta/e$ (with μ_t and μ_b the electrochemical potentials of the two superconductors). The leftmost quasiparticle path in Fig. 1, labeled a, is emitted from a filled quasielectron state in the top superconductor at an energy E between $\mu_b - \Delta$ and $\mu_b + \Delta$. This quasielectron is then reflected as a quasihole at the bottom NS interface, at an energy symmetrical about μ_b. It is then absorbed in the top superconductor where quasihole states are unoccupied at the corresponding energy (since quasielectron states are filled), and the quasiparticle path has a total length $2L$. At the energy of the initial quasielectron, the position $X = L/2$ is reached when $3/4$ of the total path remains; therefore, $f(E) = 3/4$. The second path in Fig. 1, labeled b, has length L: quasielectrons from the top superconductor with an energy between $\mu_b + \Delta$ and $\mu_t - \Delta$ are absorbed in the bottom superconductor after one traversal of the wire. Therefore $f(E) = 1/2$ at $X = L/2$. The third path, labeled c, resembles path a, with an inversion of quasiholes and quasielectrons. One obtains thus $f(E) = 1 - 3/4 = 1/4$ at the middle of the wire. Altogether, the energy distribution function at $X = L/2$ presents three steps, at $3/4$ (width 2Δ), $1/2$ (width $eU - 2\Delta$), and $1/4$ (width 2Δ). The right diagram of Fig. 1 deals with the case $\Delta < eU < 2\Delta$. The steps of $f(E)$ at $3/4$ and $1/4$ are still present, since the paths of length $2L$ of the former diagram (not reproduced here) are still relevant for the energy intervals $[\mu_b + \Delta - eU; \mu_b - \Delta + eU]$ and $[\mu_t + \Delta - eU; \mu_t - \Delta + eU]$. In addition, a new type of path appears, labeled d, with length $3L$. One obtains then three extra steps in $f(E)$, at $5/6$, $1/2$, and $1/6$. More generally, multiple Andreev reflections lead to the appearance of steps in $f(E)$ at energies between $\mu_b - \Delta$ and $\mu_t + \Delta$. The number of steps is $2 \times \text{int}(\frac{2\Delta}{eU}) + 3$, and the sum of the widths of two successive steps is eU. In the limit $U \to 0$, $f(E)$ varies linearly from 1 at $E = -\Delta$ to 0 at $E = \Delta$. To conclude, this simple model predicts a staircase pattern in the energy distribution function, which directly reveals multiple Andreev reflections.

We report results obtained on two samples, fabricated by shadow mask evaporation in order to obtain the com-

plete structure schematically described in Fig. 1. The normal metal 45-nm-thick wires are made of 99.9999% purity silver, as samples in which phase coherence lengths beyond 10 μm were found [12]. The wire length of sample No. 1 (sample No. 2) is $L = 5.15$ μm (5.6 μm), the width $w = 80$ nm (70 nm), and the normal state resistance, measured at large voltage, $R = 38$ Ω (58 Ω). The length is chosen short enough for the energy redistribution among quasiparticles to be small [13], but long enough for the density of states at the middle of the wire to be almost energy independent [2]. In sample No. 1, the wire extends at both ends into large contact pads which are covered by a 300-nm-thick aluminum layer. The reservoirs are therefore bilayers of Ag and Al and have thus a reduced superconducting gap. In sample No. 2, the contact pads have no underlying silver layer on a rectangle of 300×500 nm^2 just at the ends of the wire, in order to obtain a larger superconducting gap. A tunnel junction is formed at the middle of the wire (and, on sample No. 2, also at 1.25 μm from the top electrode), with a 100-nm-wide aluminum probe electrode. The samples were mounted in a shielding copper box on a sample holder thermally anchored to the mixing chamber of a dilution refrigerator. All connecting lines to the samples are filtered at 4.2 K and at the sample temperature. The experiment consists of measuring the differential conductance $dI/dV(V)$ of the probe junction when a voltage U is applied across the wire. Under the assumptions that the density of states of the normal wire is constant at the position of the probe junction and that the temperature of the probe electrode remains negligible compared to the critical temperature of aluminum, the differential conductance of the junction is simply a convolution product of the derivative of the density of states of the superconductor and of the distribution function in the wire [11,14]. We deconvolve the data numerically, after determining the junction resistance and gap energy at equilibrium ($U = 0$) where $f(E)$ is expected to be a Fermi function. In Fig. 2, we present with open symbols the distribution functions measured on sample No. 1 at $U = 151$ μV, 310 μV, and 595 μV, and in Fig. 3 on sample No. 2 at $U = 700$ μV, for both positions. The energy reference was taken at the potential of the center of the wire ($\mu_t = eU/2$, $\mu_b = -eU/2$). As expected from the simplified description of multiple Andreev reflections presented above, the distribution function for sample No. 1 presents, at large voltages (310 and 595 μV in Fig. 2), three steps near $\frac{3}{4}$, $\frac{1}{2}$, and $\frac{1}{4}$ (dashed lines). The distance between the center of the side steps is well given by eU. Their width gives the value of the gap in the reservoirs: $\Delta = 115$ μeV, which is as expected smaller than the gap of aluminum (200 μeV). In contrast with the simplified model, the steps are not flat, and the slope of the side steps near $3/4$ and $1/4$ is larger than the slope at $1/2$. Moreover, the model predicts five steps in $f(E)$ when U is between Δ/e and $2\Delta/e$ (see Fig. 1), whereas the data taken at $U = 155$ μV display only slight inflections of $f(E)$ around the predicted values. At voltages below 100 μV,
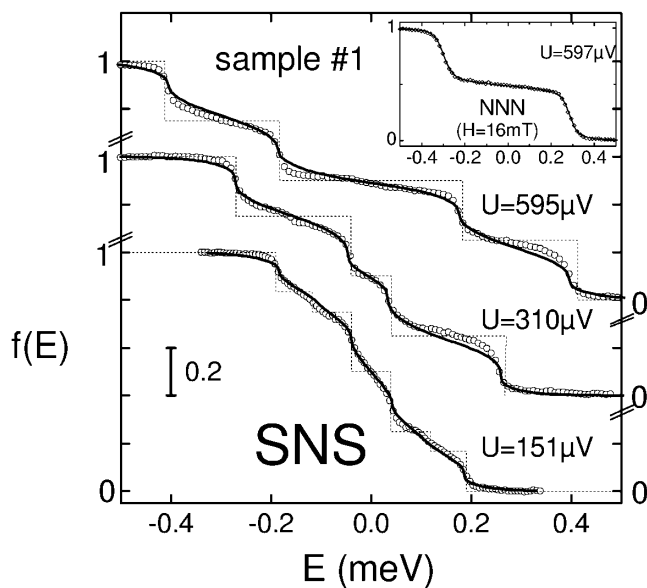
FIG. 2. Distribution functions at the middle of the wire of sample No. 1, when the reservoirs are in the superconducting state or in the normal state (inset), for different values of the bias voltage U. Symbols are experimental data, dotted lines are the expectations of the simplified theory with multiple Andreev reflections alone as in Fig. 1, and solid lines correspond to the solution of the Boltzmann equation with the Coulomb interaction term.

no structure can be seen in the distribution function, and irregularities appear in the deconvolved data, resulting from our neglection of the modification of the density of states in the wire at the scale of the Thouless energy $\hbar D/L^2$ [15] (data not shown). In sample No. 2, the evolution of the distribution function with position agrees qualitatively with the model. However, the exact position of the steps is slightly shifted from the expected values. We attribute
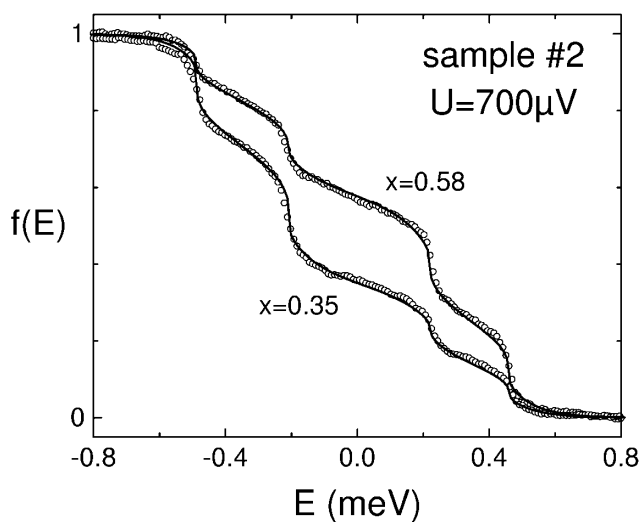
FIG. 3. Distribution functions on sample No. 2, at two positions ($x \equiv X/L = 0.58$ and $x = 0.35$), for $U = 700\ \mu$V. Symbols: experiment. Solid lines: solution of the Boltzmann equation accounting for the Andreev reflections at the reservoirs and electron-electron interactions within the wire.

this shift to the small size of the top NS contact, which introduces a significant contact resistance, accounted for by an extra length of the wire. The relative position of the probe junctions needed to explain the position of the steps in $f(E)$ turns out to be $X/L = 0.58$ (instead of 0.5) and $X/L = 0.35$ (instead of 0.25), which corresponds to an effective lengthening of the top end of the wire by about 850 nm. The widths of the side steps give slightly different gaps at both ends: 120 and 140 μeV.

In order to account for the rounding of the steps, we now include in the analysis the effect of energy relaxation of quasiparticles, due to Coulomb electron-electron [13] and electron-phonon [16] interactions. These interactions contribute to the stationary Boltzmann equation which determines the variations of $f(E)$:

$$D\frac{\partial^2 f_E}{\partial X^2} + I_{in}^{e\text{-}e}(f_E) + I_{in}^{e\text{-}ph}(f_E) = 0$$

through the interaction collision integrals [11,13]

$$I_{in}^{e\text{-}e}(f_E) = \int d\varepsilon\, dE'\, K_e(\varepsilon)$$
$$\times \{f_E \overline{f_{E-\varepsilon}} f_{E'} \overline{f_{E'+\varepsilon}} - \overline{f_E} f_{E-\varepsilon} \overline{f_{E'}} f_{E'+\varepsilon}\},$$
$$I_{in}^{e\text{-}ph}(f_E) = \int d\varepsilon\, K_{ph}(\varepsilon) f_E \overline{f_{E-\varepsilon}},$$

where $K_e(\varepsilon) = \kappa_e/\varepsilon^{3/2}$, $K_{ph}(\varepsilon) = \kappa_{ph}\varepsilon^2$ [17], f_E stands for $f(E)$, and $\overline{f_E}$ stands for $1 - f(E)$. In order to determine the Coulomb interaction parameter κ_e, we have taken advantage in sample No. 1 of the weaker superconductivity in the reservoirs than in the probe finger, which allows one to turn just the reservoirs normal in a moderate magnetic field ($H = 16$ mT, applied perpendicular to the sample plane), while keeping the probe superconducting. The distribution function with normal reservoirs at $U = 595\ \mu$V is displayed in the inset in Fig. 2, and has, as expected [11], only one step near $1/2$. From the fit of a set of such curves at different values of U, we have confirmed the ε dependence of $K(\varepsilon)$ and obtained [13] $\kappa_e = 0.75$ meV$^{-1/2}$ ns^{-1}. The coupling constant κ_{ph} between electrons and phonons was extracted from the temperature dependence of the phase coherence time on similarly fabricated silver samples [12]: $\kappa_{ph} = 8$ meV^{-3} ns^{-1}. When the reservoirs are superconducting, the same Boltzmann equation also allows one to compute numerically $f(E)$, with the following boundary conditions for $|E| < \Delta$: (a) $f(\mu + E) = 1 - f(\mu - E)$ accounts for the equality of the occupancy of quasielectron and quasihole states at symmetric energies about the electrochemical potential μ of the superconductor and (b) $\frac{\partial f}{\partial x}(\mu + E) = -\frac{\partial f}{\partial x}(\mu - E)$ is the conservation of the quasiparticle current. The results for $f(E)$, using the value of κ_e and κ_{ph} given above, are plotted with solid lines in Fig. 2. Note that the inclusion of the phonon term $I_{in}^{e\text{-}ph}(f)$ changes only slightly $f(E)$. The side steps at $\frac{3}{4}$ and $\frac{1}{4}$ are more rounded than the step at $\frac{1}{2}$, as observed.

Indeed, they correspond to quasiparticles staying in the wire 4 times longer on average (path length $2L$), which are thus more likely to interact with other quasiparticles. The distribution function at $U = 151$ μV is very rounded by interactions, as expected for quasiparticle paths with lengths $2L$ and $3L$. The overall agreement with the measurements indicates that this simple picture of multiple Andreev reflections [i.e., with assumptions (ii) and (iii)] together with Coulomb interactions captures the essential phenomena. In sample No. 2, a good fit of the data is found with $\kappa_e = 0.35$ meV$^{-1/2}$ ns^{-1} at both measuring positions (see solid curves in Fig. 3).

We now discuss the influence of a more precise description of Andreev reflection, i.e., when relaxing assumptions (ii) and (iii). This can be achieved using the Usadel equations [5], assuming that the wire is long enough so that the superconducting correlations are completely lost in the middle of the wire [18], and neglecting electron-electron interactions. Qualitatively, in the example of trajectory a in Fig. 1, the time spent near the bottom NS interface is shortened by the renormalization of the diffusion constant at energies close to the electrochemical potential of the superconductors [3], which results in a shorter remaining length when $X = L/2$ and thus to a value for $f(E)$ smaller than 3/4. However, in our experiment, where the length of the wire is 1 order of magnitude larger than the superconducting coherence length $\sqrt{\hbar D/\Delta}$, this effect on $f(E)$ turns out to be negligible.

To conclude, our measurements display clear signatures of multiple Andreev reflections in SNS junctions and demonstrate the importance for the proximity effect of electron-electron interactions, a contribution which is not taken into account in the standard Usadel formalism.

---

[1] B. Pannetier and H. Courtois, J. Low Temp. Phys. **188**, 599 (2000), and references therein.

[2] S. Guéron, H. Pothier, N. O. Birge, D. Esteve, and M. H. Devoret, Phys. Rev. Lett. **77**, 3025 (1996).

[3] H. Courtois, P. Charlat, Ph. Gandit, D. Mailly, and B. Pannetier, J. Low Temp. Phys. **116**, 187 (1999).

[4] P. Dubos, H. Courtois, B. Pannetier, F. K. Wilhelm, A. D. Zaikin, and G. Schön, cond-mat/0008146.

[5] A. Schmid, in *Nonequilibrium Superconductivity, Phonons, and Kapitza Boundaries,* edited by K. E. Gray (Plenum Press, New York, 1981), p. 423; J. Rammer and H. Smith, Rev. Mod. Phys. **58**, 323 (1986); A. I. Larkin and Yu. N. Ovchinikov, in *Nonequilibrium Superconductivity,* edited by D. N. Langenberg and A. I. Larkin (North-Holland, Amsterdam, 1986), p. 493; K. D. Usadel, Phys. Rev. Lett. **25**, 507 (1970).

[6] C. Strunk, T. Hoss, T. Nussbaumer, and C. Schönenberger, in *Quantum Physics at Mesoscopic Scale,* edited by C. Glattli, M. Sanquer, and J. Trân Thanh Vân, Series Moriond Condensed Matter Physics (Editions Frontières, Gif-sur-Yvette, France, 1999).

[7] E. Scheer, N. Agrait, J.-C. Cuevas, A. Levy Yeyati, B. Ludoph, A. Martin-Roderos, G. R. Bollinger, J. M. van-Ruitenbeek, and C. Urbina, Nature (London) **394**, 154 (1998).

[8] R. Cron, M. F. Goffman, D. Esteve, and C. Urbina (to be published).

[9] M. F. Goffman, R. Cron, A. Levy Yeyati, P. Joyez, M. H. Devoret, D. Esteve, and C. Urbina, Phys. Rev. Lett. **85**, 170 (2000).

[10] A. Furusaki and M. Tsukada, Solid State Commun. **78**, 299 (1991); C. W. J. Beenakker and H. van Houten, Phys. Rev. Lett. **66**, 3056 (1991).

[11] H. Pothier, S. Guéron, Norman O. Birge, D. Esteve, and M. H. Devoret, Phys. Rev. Lett. **79**, 3490 (1997).

[12] A. B. Gougam, F. Pierre, H. Pothier, D. Esteve, and N. O. Birge, J. Low Temp. Phys. **118**, 447 (2000).

[13] F. Pierre, H. Pothier, D. Esteve, and M. H. Devoret, J. Low Temp. Phys. **118**, 437 (2000).

[14] J. M. Rowell and D. C. Tsui, Phys. Rev. B **14**, 2456 (1976).

[15] When heating the sample, the conductance peak at Δ/e in the $dI/dV(V)$ characteristic taken at $U = 0$ split into two peaks, as expected from the presence of a minigap in the density of states in the wire [see W. Belzig, C. Bruder, and A. L. Fauchere, Phys. Rev. B **58**, 14 531 (1998); F. K. Wilhelm and A. A. Golubov, Phys. Rev. B **62**, 5353 (2000)].

[16] The collision term corresponding to phonon emission is important for data taken on long wires at large voltages. The addition of this term to the electron-electron collision term in the Boltzmann equation suffices to account for the measured distribution functions in silver wires, without any *ad hoc* assumption [13].

[17] The ε^2 dependence of the electron-phonon interaction kernel is equivalent to the T^3 dependence of the energy transfer rate between electrons and phonons reported, for example, in M. L. Roukes, M. R. Freeman, R. S. Germain, R. C. Richardson, and M. B. Ketchen, Phys. Rev. Lett. **55**, 422 (1985).

[18] E. V. Bezuglyi, E. N. Bratus', V. S. Shumeiko, G. Wendin, and H. Takayanagi, Phys. Rev. B **62**, 14 439 (2000).